

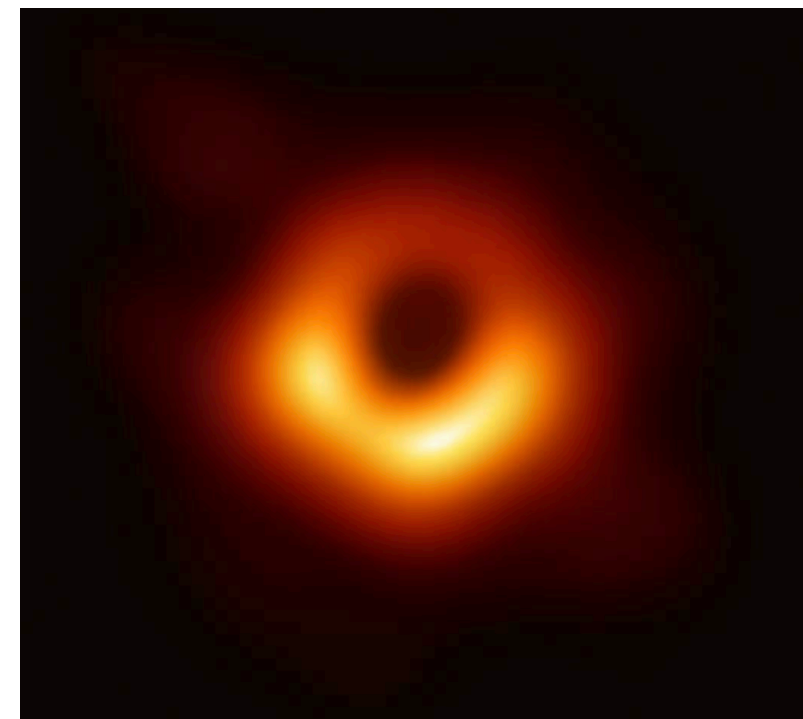
# MRI in Rotating Flows: Implications for the Solar Tachocline and Dynamo Processes

Ashish Mishra, George Mamatsashvili, Frank Stefani

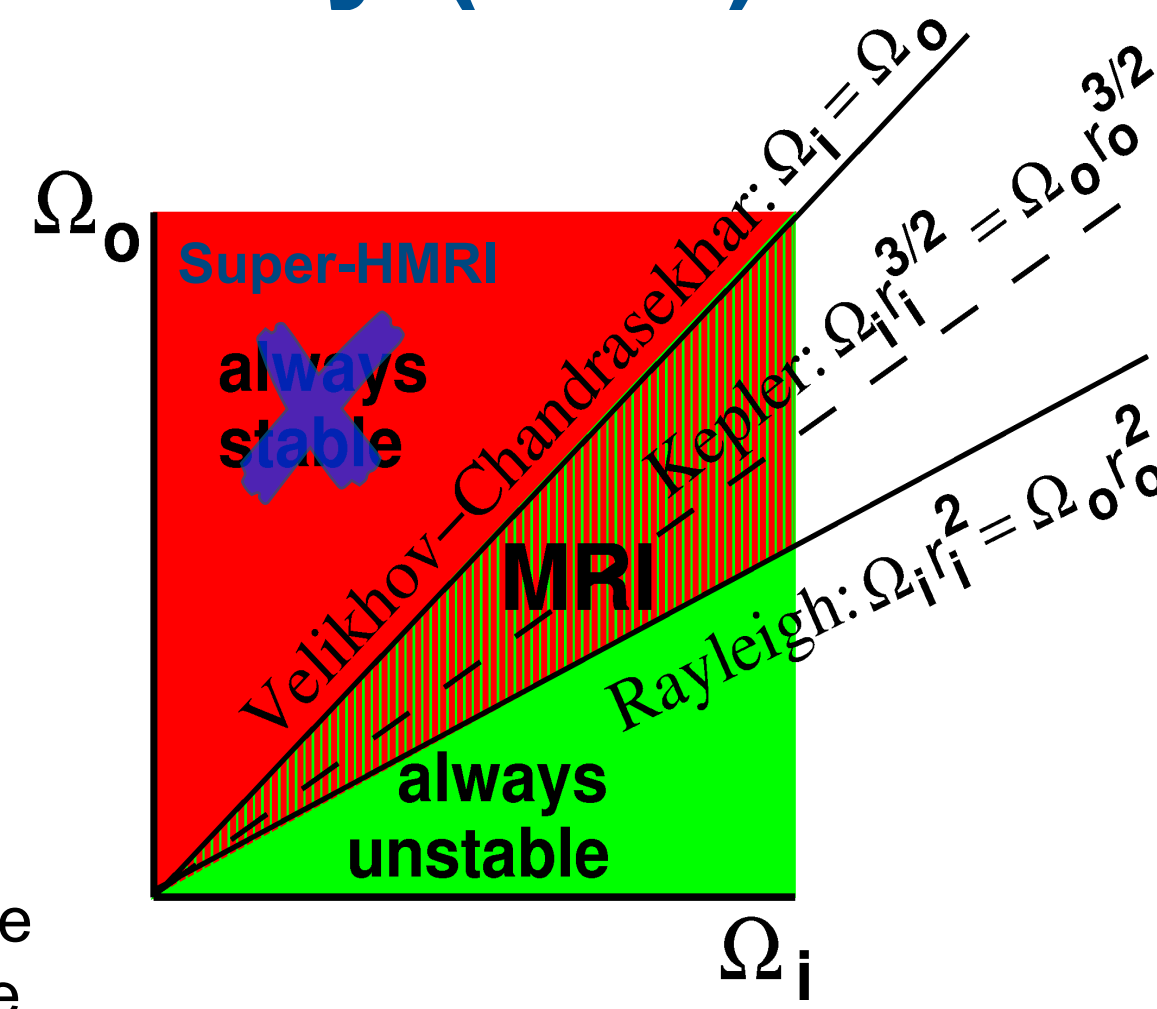
## Magnetorotational instability (MRI)



Accretion disks around black hole (NASA)



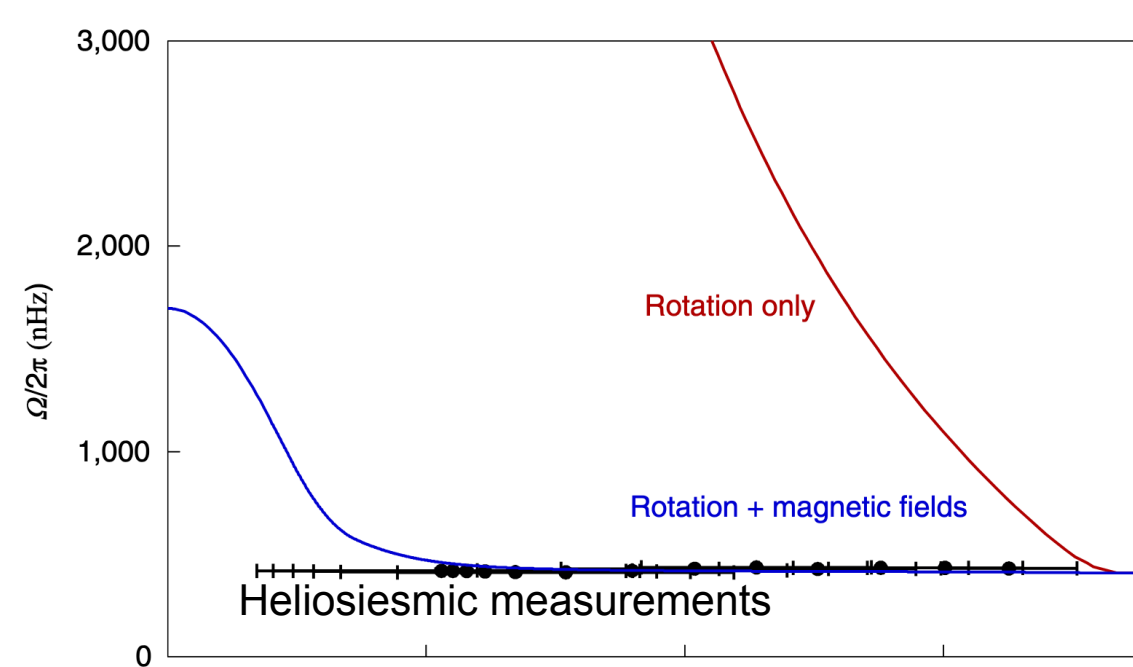
Observation of M87 black hole from Event Horizon Telescope



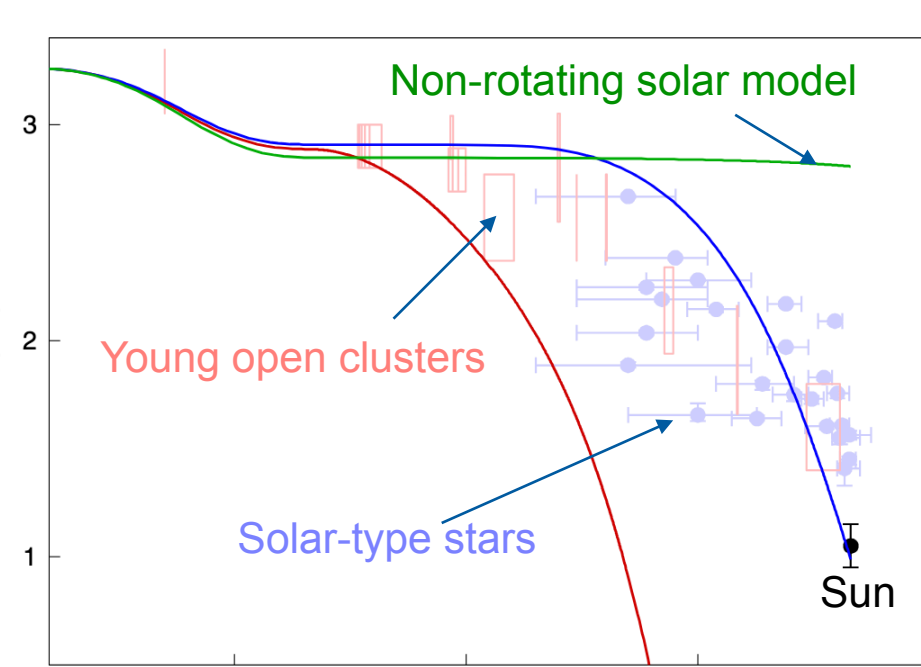
- **Magnetorotational instability (MRI)** is a powerful dynamical instability in rotational flows arising as a result of the combined action of differential rotation (shear) of the flow and an anchored magnetic field.

- MRI is amongst the most important instabilities in astrophysics, driving angular momentum and mass transport in various cosmic objects and can drive dynamo action.

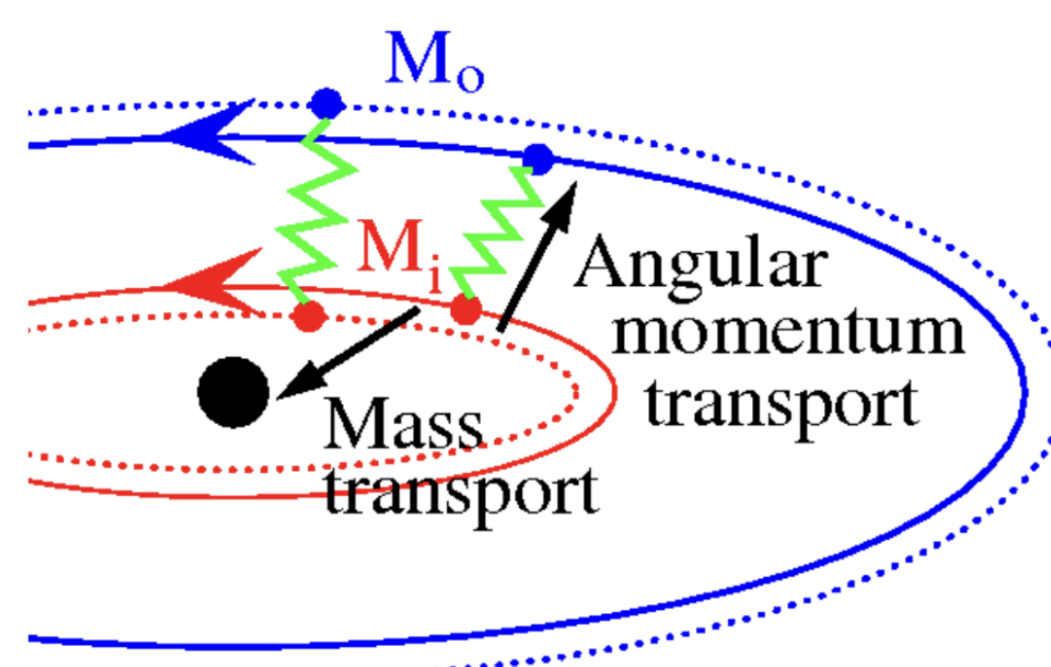
- **Relevance to the Sun:** MRI may also explain  $^7\text{Li}$  mixing and angular momentum transport in the solar tachocline. [Meduri et al., A&A.683, A12 \(2024\)](#)



Rotation profiles in the solar radiative interior



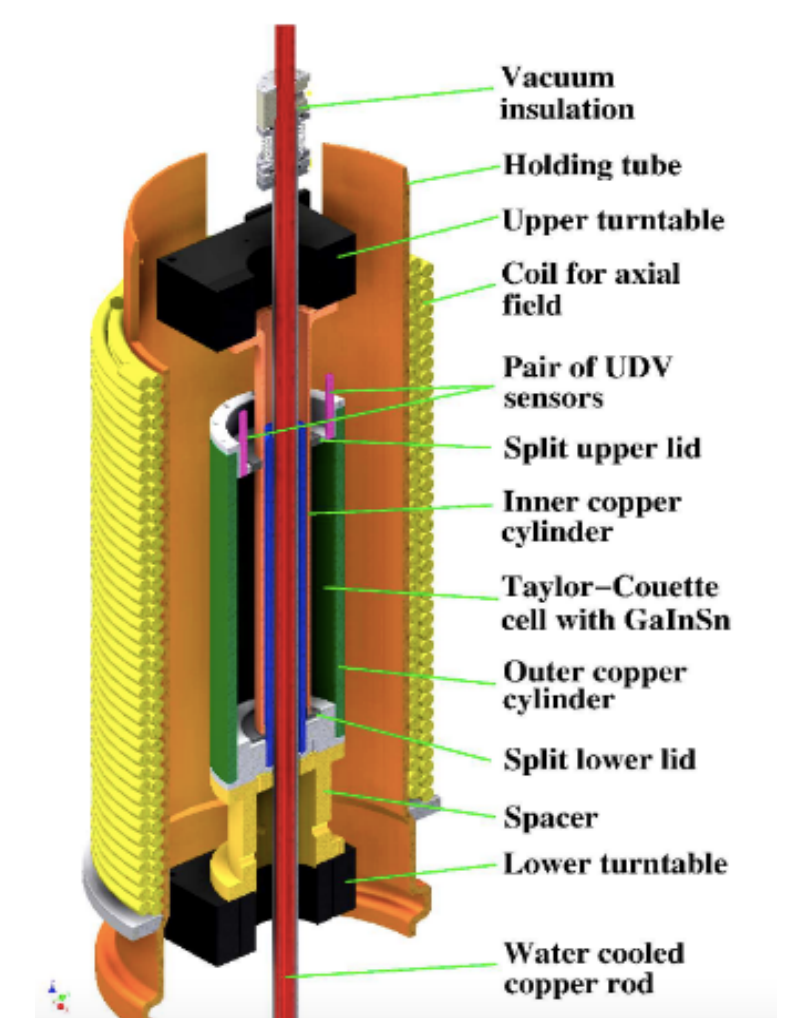
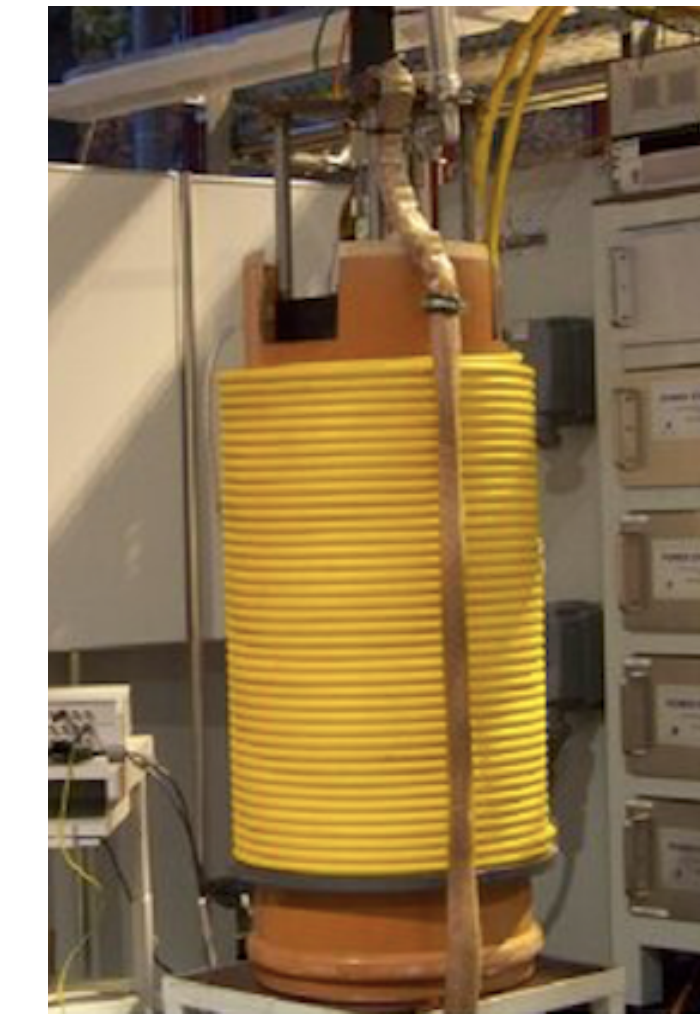
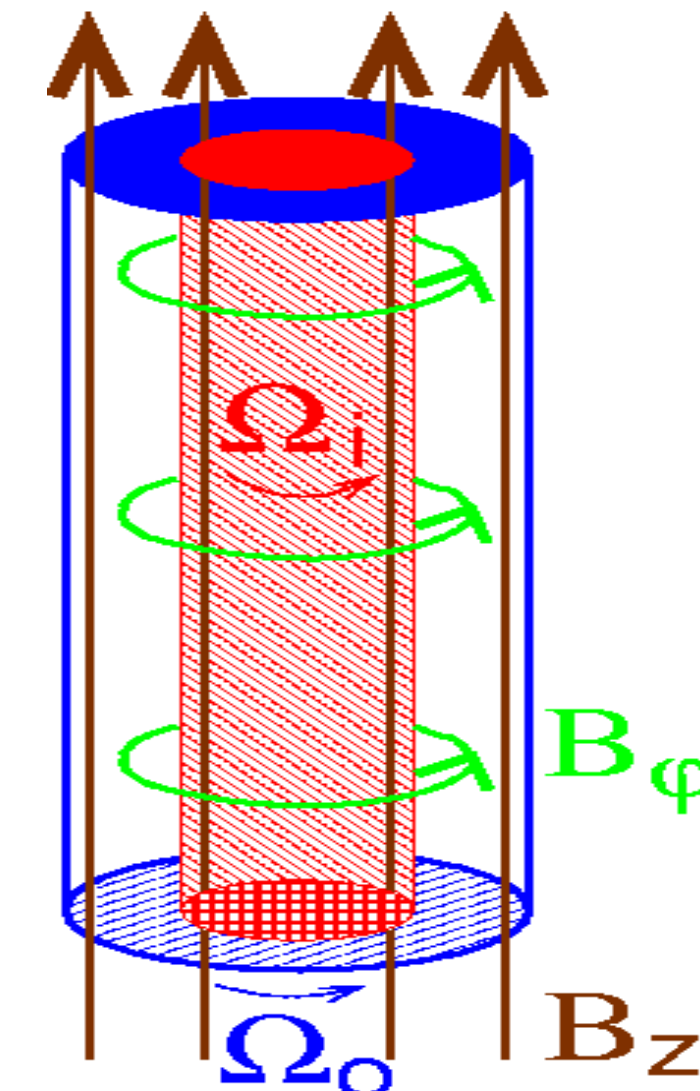
Lithium surface abundance as a function of age for different solar models. [Eggenberger et al., Nature Astron. 6, 788 \(2022\)](#)



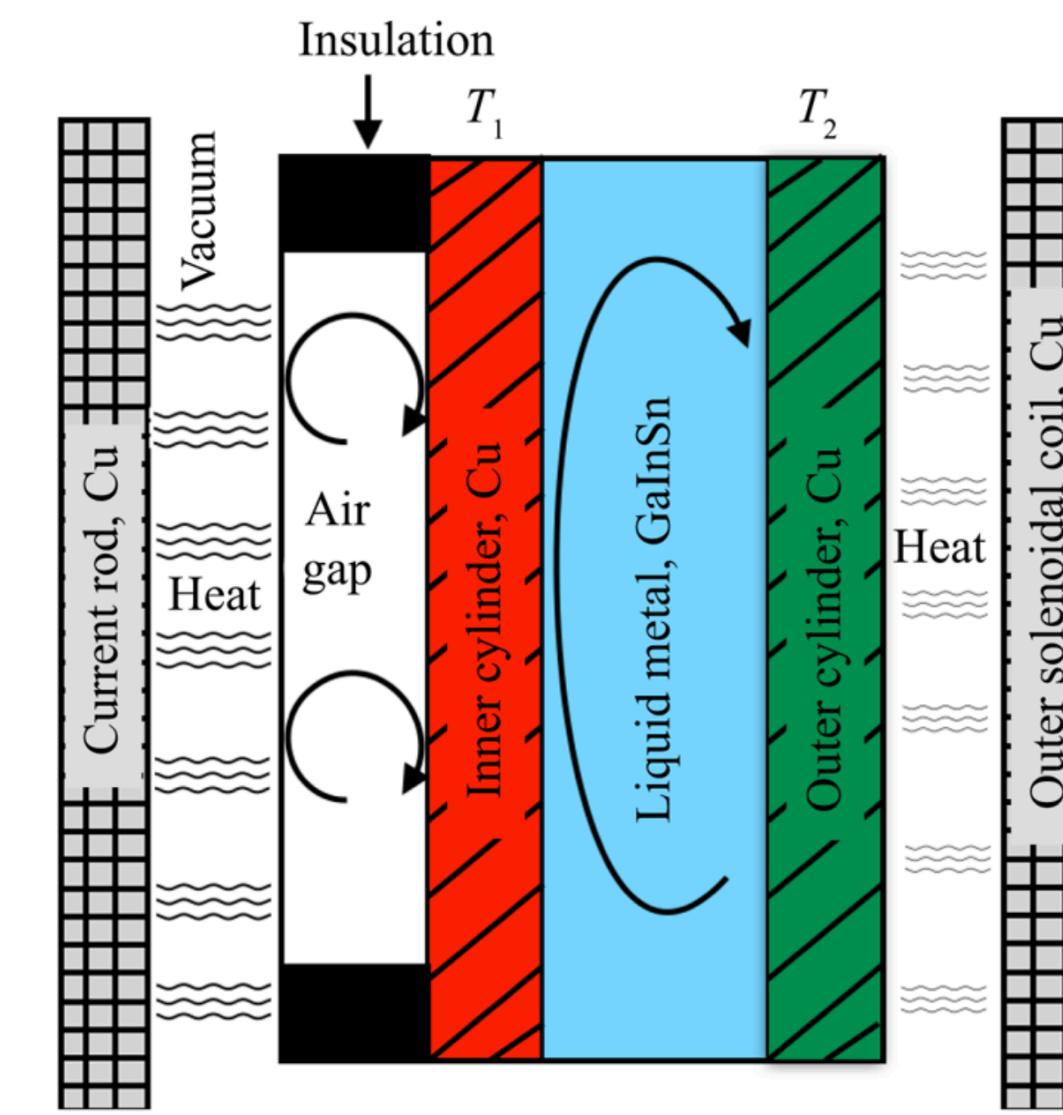
Spring-Mass analogy of MRI

## MRI in the lab — PROMISE experiment

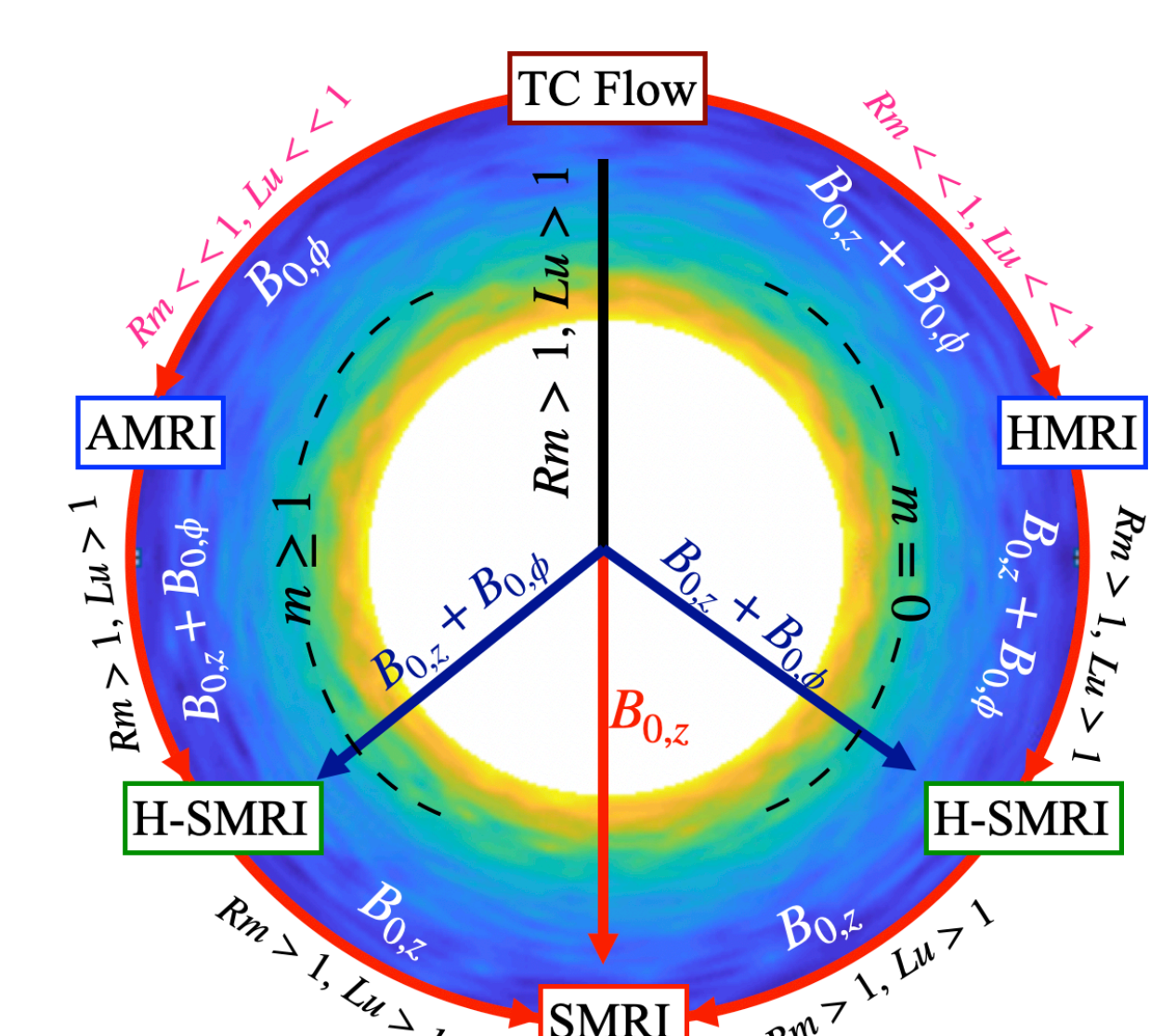
Taylor-Couette (TC) flow of a liquid metal between two coaxial rotating cylinders subject to external azimuthal  $B_\phi$  and axial  $B_z$  magnetic fields is, due to its analogy with accretion disks, a basic experimental setup to detect and study MRI in the lab.



**PROMISE** (Potsdam ROssendorf Magnetic InStability Experiment) facility at HZDR consisting of a TC device filled with galinstan (GaInSn).



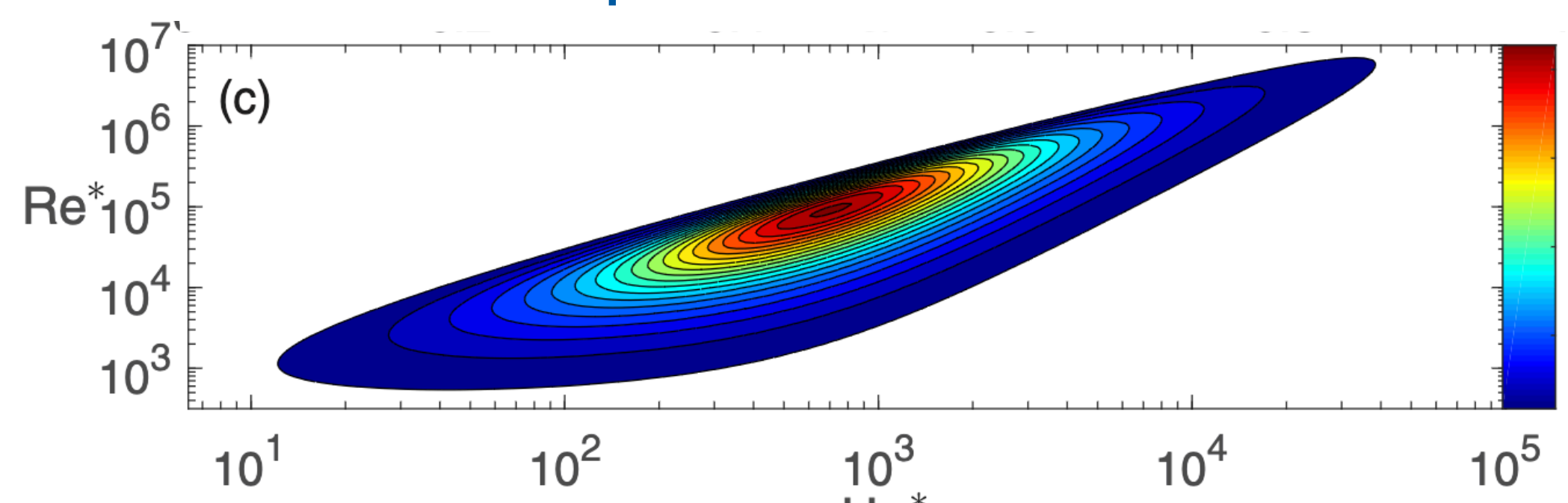
First experiment to incorporate magnetic field, rotation and thermal convection.



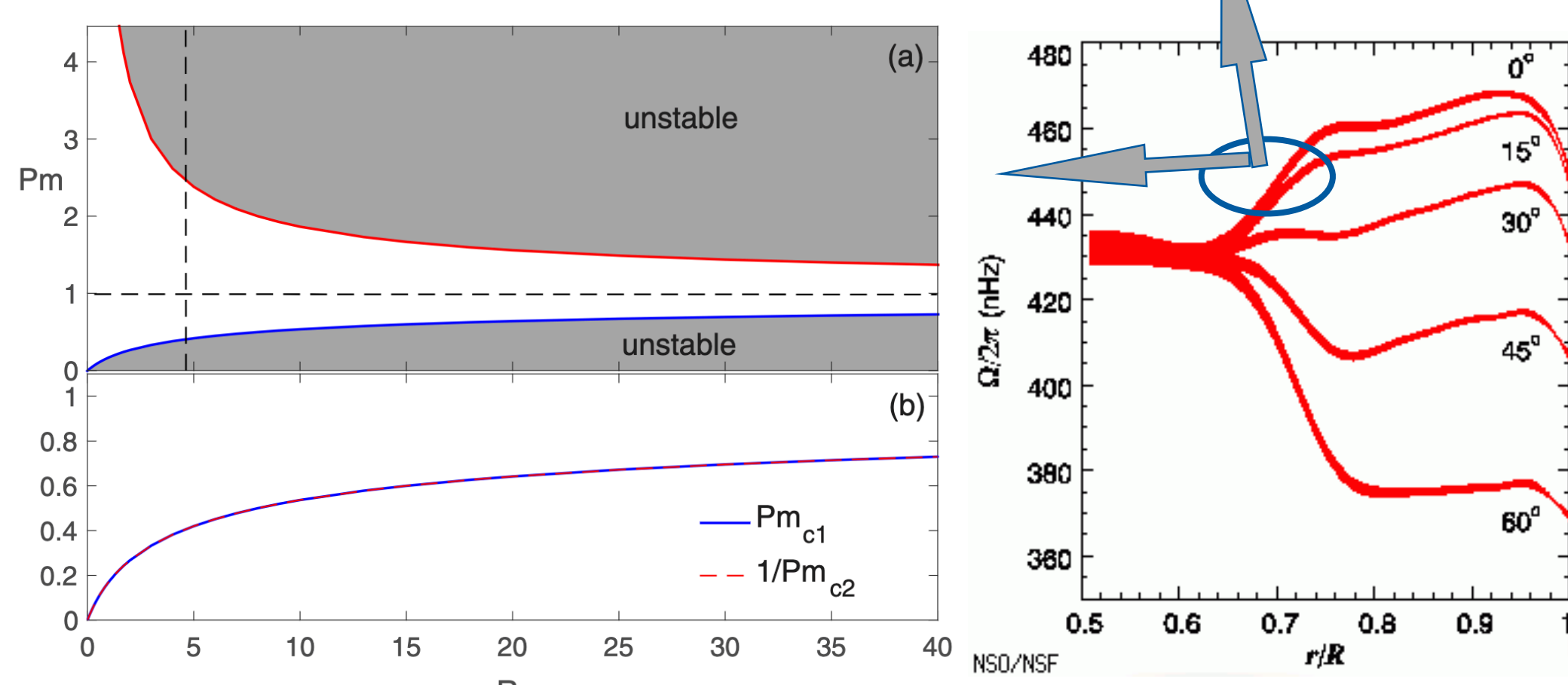
MRI and its variants in TC device

## MRI Variants and Angular Momentum Transport in the Solar Interior

### Super-Helical MRI



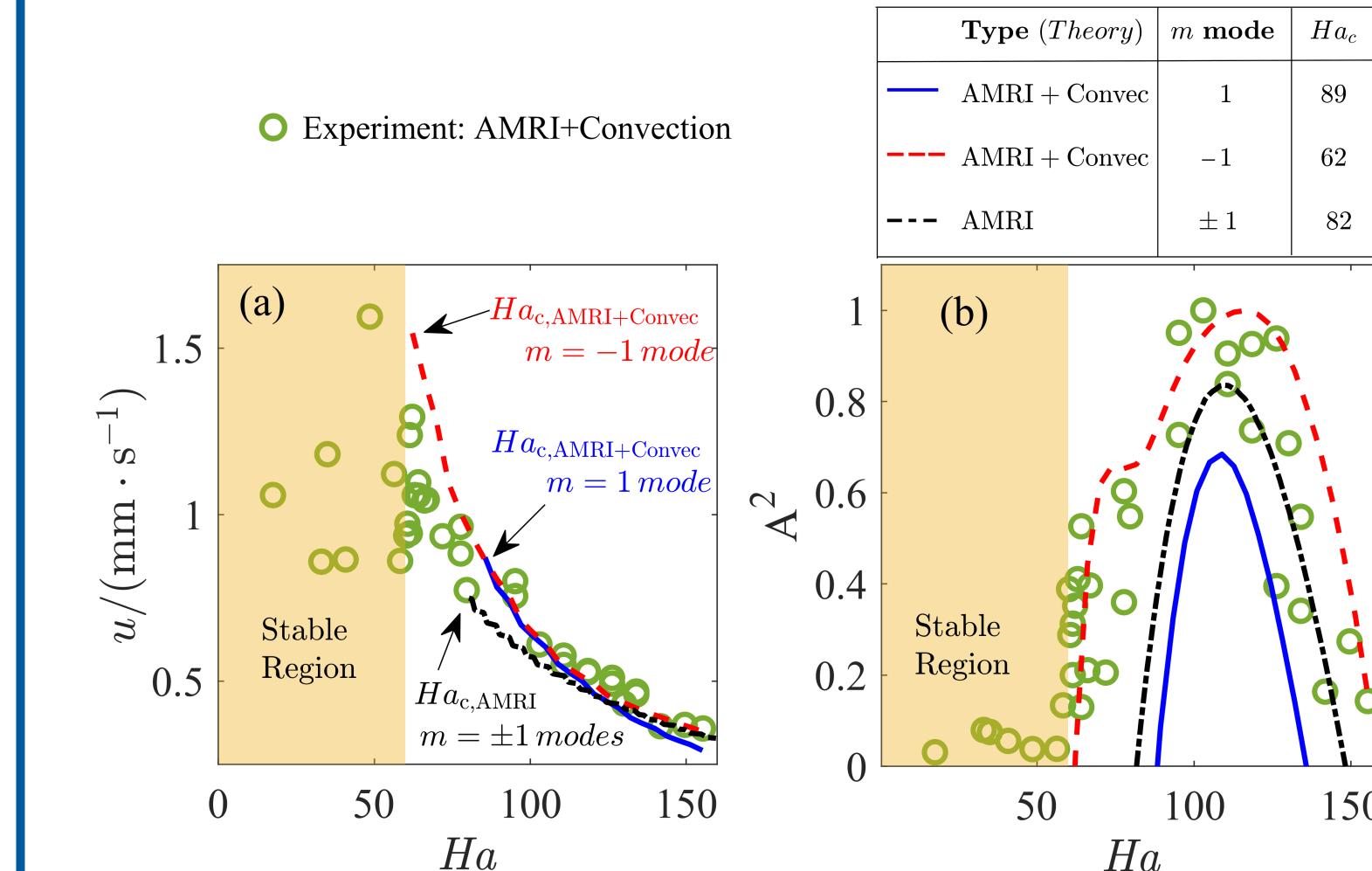
Instability growth rate as a function of  $Ha^*$  and  $Re^*$  at  $Ro = 1.5$  and  $Pm = 10^{-6}$ .



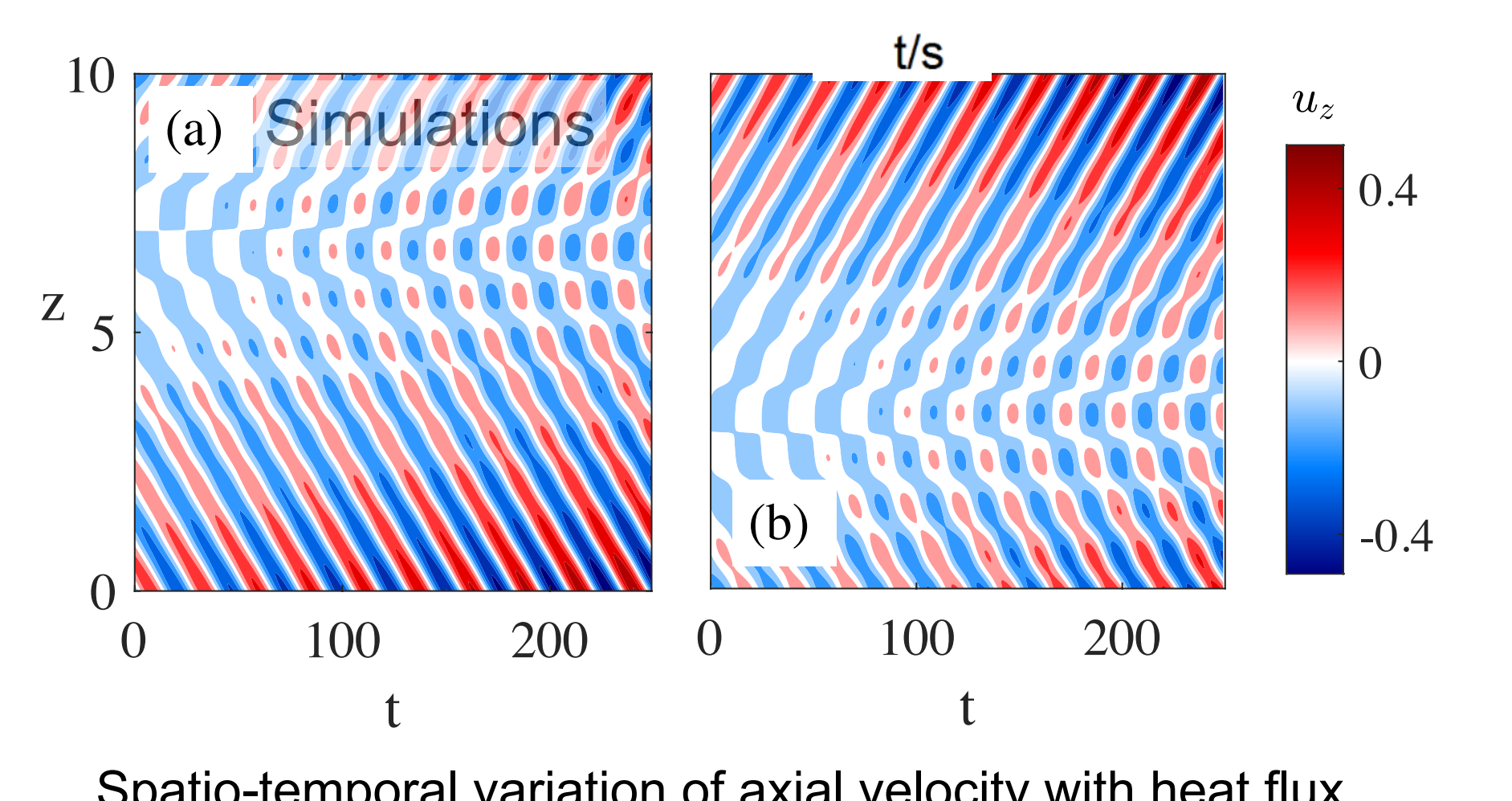
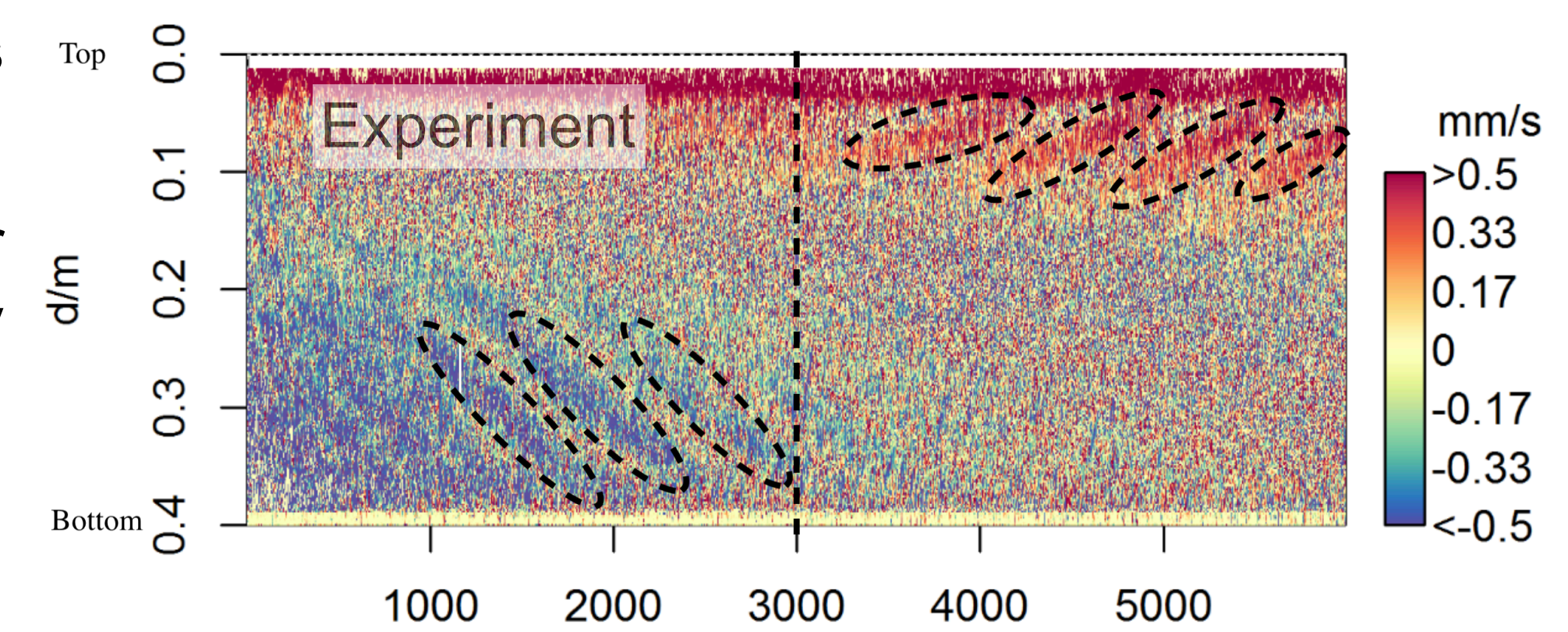
Super-HMRI (grey) at radially increasing angular velocity, or positive shear. [Mamatsashvili et al., PRF. 4, 103905 \(2019\)](#)

### Azimuthal MRI in the presence of thermal convection

- MRI in the presence of thermal convection is experimentally explored for the first time.
- We show that the critical Hartmann number ( $Ha$ ) for the onset of AMRI is reduced by convection.
- Convection breaks symmetry between  $m = \pm 1$  modes of Azimuthal MRI.

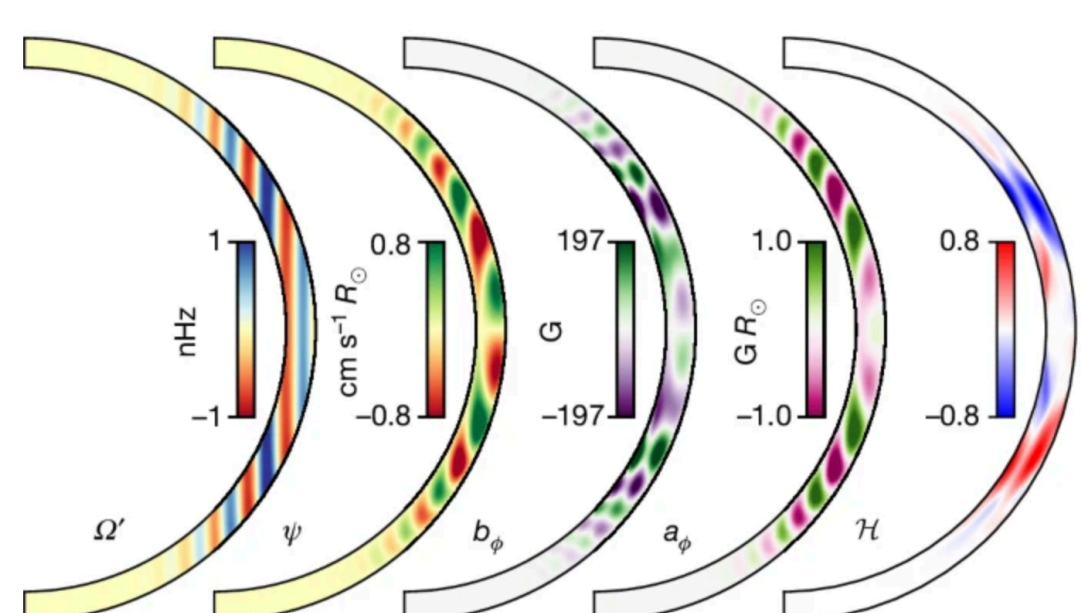


(a) Phase velocities and (b) normalized energy content  $A^2$  of the absolute AMRI in the presence of convection at  $Re=1480$ .



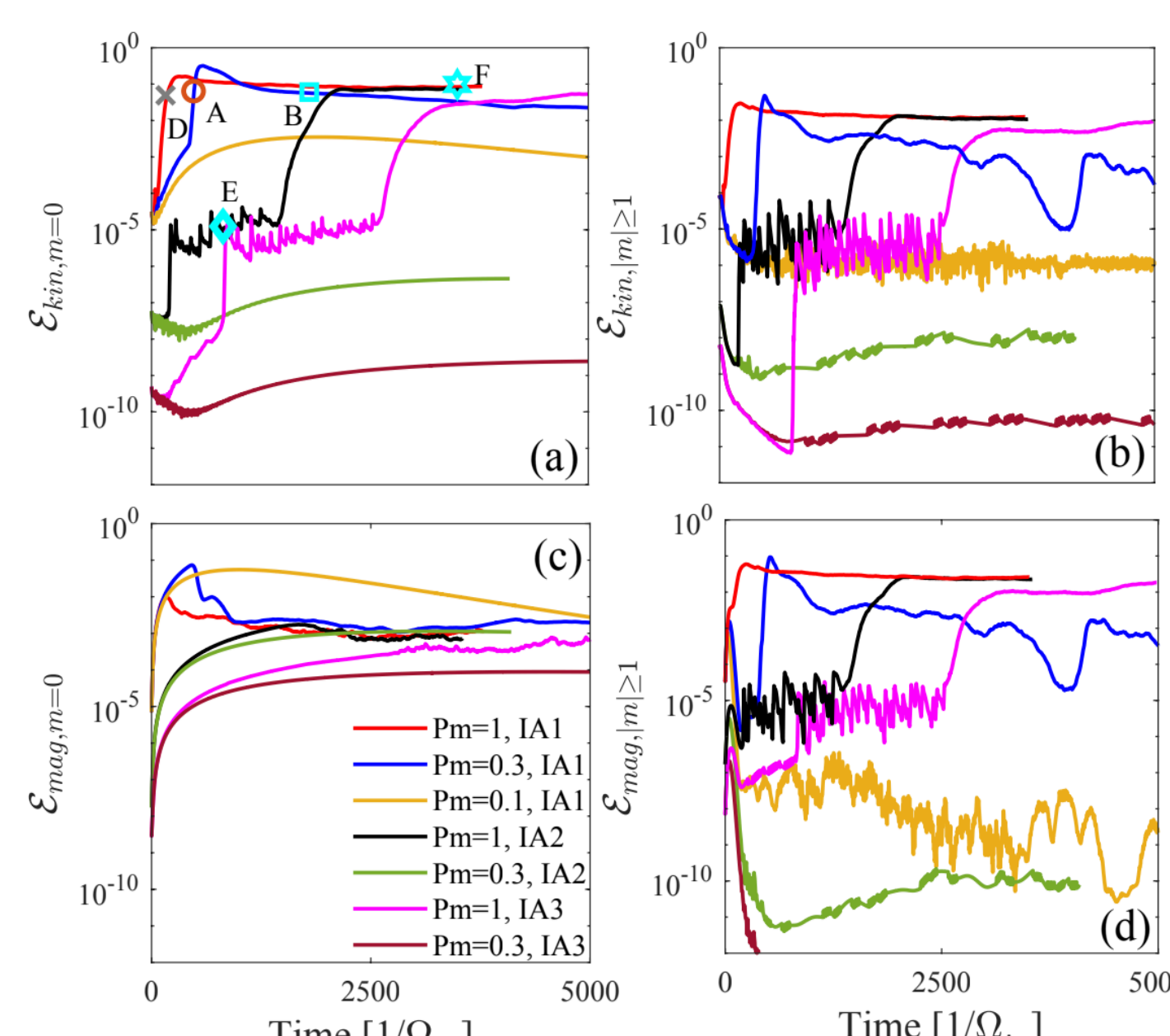
Spatio-temporal variation of axial velocity with heat flux direction (a) outer to inner cylinder and (b) inner to outer cylinder. [Mishra et al., JFM, 992:R1, \(2024\)](#)

## MRI-driven magnetic dynamo at small magnetic Prandtl number ( $Pm \leq 1$ )

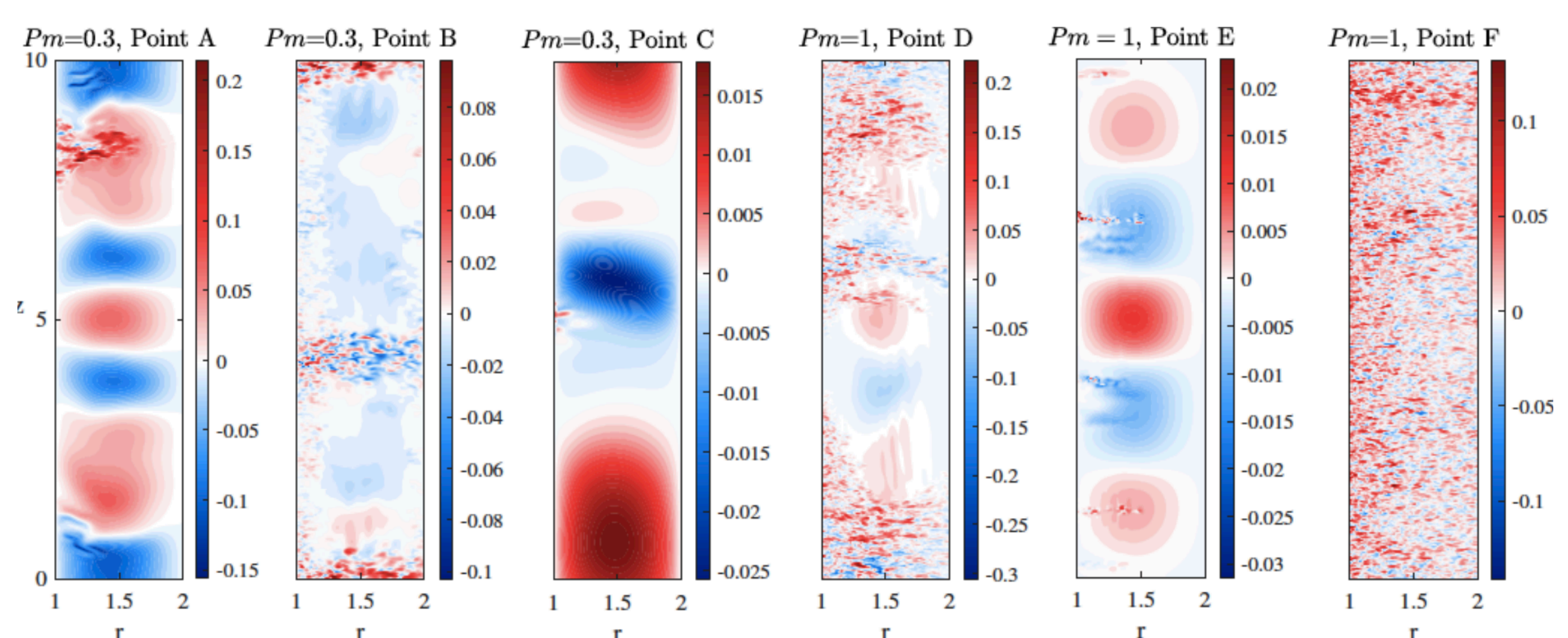


Solar dynamo driven by MRI starts near the surface. [Vasil et al., Nature, \(2024\)](#)

- MRI driven dynamo amplifies and sustains large-scale magnetic fields.
- We demonstrate the existence of a nonlinear MRI-driven dynamo in a TC flow at low magnetic Prandtl numbers ( $Pm \leq 1$ ), relevant to solar conditions where  $Pm$  is typically very small.



Evolution of kinetic and magnetic energy at different initial amplitude and  $Pm$ .



Structure of the azimuthal field  $B_\phi$  in the  $(r, z)$ -plane at a given azimuthal angle  $\phi$  and the characteristic time moments A, B, C for  $Pm = 0.3$  and D, E, F for  $Pm = 1$ . Namely, the moments A and D correspond to the growth stages, while the moments B and F to the strong and the moments C and E to the weak dynamo states. [Mishra et al., PRL, under revision \(2025\)](#)